PRAMANA
— journal of
physics

Vol. 60, No. 4
April 2003
pp. 687–696

A survey of lattice results on finite temperature quantum chromodynamics

E LAERMANN
Fakultät für Physik, Universität Bielefeld, D-33615 Bielefeld, Germany

Abstract. The talk summarizes some new results of lattice investigations of QCD at finite temperature. The topics discussed cover the flavor dependence of the critical temperature and the equation-of-state as well as hadronic correlation functions.

Keywords. Quantum chromodynamics; finite temperature.

PACS Nos 11.15.Ha; 12.38.Gc; 12.38.Mh

1. Introduction

Numerical calculations in the framework of lattice regularized QCD have proven to provide valuable information on the thermodynamics of quarks and gluons at high temperature. In particular, this is true for simulations of the pure gluon theory, the so-called quenched approximation of QCD. Here, the bulk thermodynamic properties are well-known and established: the value of the critical temperature T_c for the transition from the hadronic to the plasma phase of QCD has been determined with 2–3% uncertainty, the transition itself is of first order with known critical exponents and the equation-of-state has been consistently computed with various discretizations. These results are available with all systematic errors due to finite volume and finite lattice spacing under control. These computations have shown that non-perturbative effects prevail up to quite high temperatures. On the other hand, they demonstrated what can be gained from improved discretization schemes in which the effects of finite lattice spacing are reduced by construction.

The analysis of full QCD with the inclusion of dynamical quarks has not yet reached a similarly satisfying precision. This is largely due to the enormously increased demand on computational power. In particular, if one is aiming at simulations at physical, small quark masses the computational effort needed is larger by orders of magnitude. Moreover, simple model as well as numerical calculations quite clearly point to a value of T_c which is decreasing with smaller quark masses. Since the UV cut-off effects induced by non-vanishing lattice spacing a are controlled by the dimensionless number $aT = 1/N_\tau$ this decrease in T_c leads to an even higher computational effort which depends on the number of lattice points in the temporal (temperature) direction N_τ to some large power. Finally, standard (staggered or Wilson) discretizations of fermions on the lattice destroy some chiral and/or flavor symmetries which are recovered only in the continuum limit $a \to 0$. In order to approximate continuum physics already at larger lattice spacings improvements of the standard actions as well as the development of chiral actions as domain wall or the so-called overlap formulations are being discussed intensely at recent lattice conferences. However, since these topics are of rather lattice-technological importance at the moment I will not discuss them here but concentrate on the presentation of some results of phenomenological nature obtained so far. In the next section I will summarize the present knowledge about the phase diagram and the critical temperature in the presence of two to three light dynamical quarks. This is followed by a presentation of the results obtained for pressure and energy density as a function of temperature, again for QCD with two and three light flavor degrees of freedom. Section 4 elaborates on some recent results on hadronic excitations at high temperature.

2. Critical temperature and the phase transition

The nature of the chiral phase transition is expected to be strongly dependent on the number of light quark flavors. These expectations are summarized in figure 1. Since the physics at the transition is governed by long ranged correlations, the expectations are borne out of studies of the global chiral symmetries of the QCD action and the properties of systems with the same invariances. For two flavors, the global chiral symmetry of the QCD action is isomorphic to $O(4)$. In analogy to the $O(4)$ sigma model, one therefore expects [1] a continuous transition with $O(4)$ critical properties in the chiral limit. This holds unless the anomalous $U_A(1)$ of QCD is effectively restored at or even below T_c in which case a first-order chiral transition may be realized. All presently available lattice results support a continuous behavior. Moreover, the $U_A(1)$ does not seem to be restored at the critical temperature [2]. Regarding the critical behavior, however, the situation is not yet conclusive. Studies of the quark mass dependence of various susceptibilities [3,4] are in conflict with the predicted $O(4)$ critical exponents. The same conclusion is drawn from an investigation of the (infinite volume) magnetic equation of state [5]. Both analyses are based on the staggered discretization. In contrast, computations of the magnetic equation of state with Wilson quarks [6] support $O(4)$ critical behavior. These findings are not simply explained by the different discretizations chosen as a recent finite size scaling analysis [7] of the magnetic equation of state, although working with staggered quarks, also shows consistency with $O(4)$ behavior. Quite clearly, the solution of this puzzling situation requires further dedicated work.

For three-degenerate light quark, again from symmetry reasons, one expects a first-order transition. The line of first-order transitions should extend from the chiral limit to an end point at some non-zero quark mass where the transition becomes continuous and is expected to lie in the Ising universality class [8]. A recent lattice simulation [9] supports this picture even with respect to the universality class. The location of the end point, however, is not a universal property and the current estimates [10,9] vary between values of 190 and 260 MeV for the corresponding pseudoscalar mass, depending on the action chosen.

Thus, the second-order end point has not yet unambiguously been fixed in physical units for three-degenerate quarks. This holds even more so for the line of second-order end points in the case of non-degenerate quark masses. Older results suggested that the physically realized point might be in the cross-over region. However, the physical values for

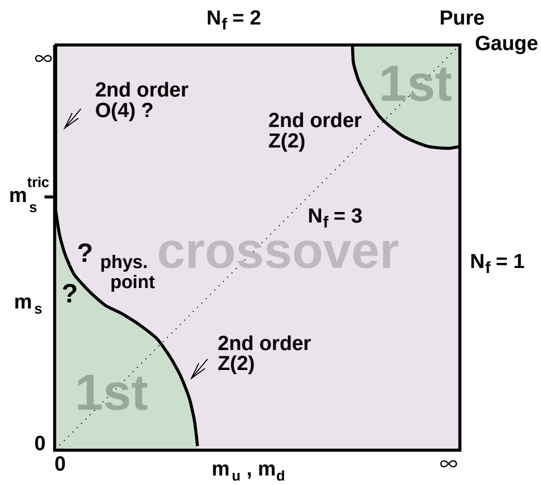

Figure 1. The expected phase diagram in the plane of strange and u, d quark masses.

the quark masses are not yet really known to a high precision and moreover it is difficult to simulate at all three quark masses dialed to the right values. Since the physical point might well be in either region, two- as well as three-degenerate flavor dominated simulations are being carried out for both cases, $N_{\rm F} = 2$ and $N_{\rm F} = 3$, supplemented by studies with non-degenerate flavors, two light and one heavier ($N_{\rm F} = 2+1$) quark.

The current results for the critical temperature are summarized in figure 2. The figure on the left contains data [11–15] for two flavors, all obtained with improved actions. Discrepancies between Wilson and staggered quarks seen in earlier computations with standard discretizations are greatly reduced. $T_{\rm c}$ vs. the zero-temperature pseudoscalar mass is plotted as a measure of the quark mass, both in units of the vector meson mass. Note that the strong decrease of the ratio $T_{\rm c}/m_{\rm V}$ with increasing quark mass is due to the rising vector meson mass which diverges in the infinite quark mass limit $m_{\rm PS}/m_{\rm V} \to 1$. It should also be noted that close to the chiral limit two conflicting quark mass dependencies should influence the ratio $T_{\rm c}/m_{\rm V}$: the vector mass should increase linearly with the quark mass leading to a decrease of the ratio as the square root of the pseudoscalar mass. This is counteracted by the quark mass dependence of $T_{\rm c}$ itself for which the analogy with $O(4)$ suggests a behavior $\sim m_{\rm q}^{1/\beta\delta} \sim m_{\rm PS}^{1.1}$. Thus, at small enough quark and pseudoscalar mass resp. a linear decrease towards the chiral limit is expected to win. This effect is not yet seen.

A scale for $T_{\rm c}$ much less affected by the quark mass than the vector meson mass is the string tension which is used on the right-hand side. Indeed, this figure shows that the critical temperature is decreasing with decreasing quark mass. The decrease appears to be compatible with a linear dependence on the pseudoscalar mass as expected for $N_{\rm F} = 2$. The linear dependence, however, also seems to hold for three-degenerate quarks. Note also, that $T_{\rm c}$ is reduced half way down from the quenched value, shown as the band to the very right of the figure, already at a pseudoscalar mass as large as 1500 MeV. It is thus not the chiral dynamics which controls the critical temperature and one may speculate that a resonance gas picture is more appropriate to describe the thermodynamics close to $T_{\rm c}$. The overall quark mass dependence for both two- and three-flavors is rather weak and, as

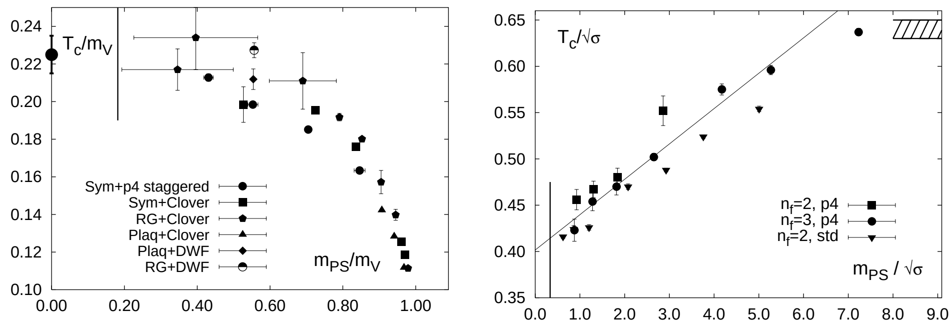

Figure 2. The critical temperature. On the left, T_c is given in units of the vector meson mass. The results [11–15] originate from a variety of improved actions for $N_F = 2$. On the right, results [11] for 2 and 3 improved $(p4)$ staggered quarks are compared to $N_F = 2$ standard (std) simulations, all normalized to the string tension.

noted already, compatible with a behavior linear in the pseudoscalar mass. The difference between $N_F = 2$ and 3 is small and amounts to about 20 MeV, independent of the quark mass. Extrapolating the shown results to the chiral limit, one obtains $T_c = 154 \pm 8$ MeV for $N_F = 3$ and 173 ± 8 MeV for $N_F = 2$ improved staggered quarks [11]. The latter value is in staggering agreement with the result from an analysis with two flavors of clover-improved Wilson quarks [13], $T_c = 171 \pm 4$ MeV. The errors are statistical only and cannot account for the possible yet unknown systematic errors originating from the fact that the simulations have been carried out on lattices with $N_\tau = 4$ which corresponds to a rather large lattice spacing of about 0.3 fm. However, in both simulations improved actions have been used.

3. Equation of state

Energy density $\varepsilon(T)$ and pressure $p(T)$ are fundamental thermodynamic quantities governing the evolution of the plasma once being created in heavy-ion collisions. Their determination on the lattice is strongly affected by the UV cut-off introduced through the finite lattice spacing. As perturbative (lattice) calculations reveal, this effect is even more pronounced in the presence of dynamical quarks. Since on the other hand the signal for these quantities reduces proportional to a^4 the use of improved actions which are designed to reduce the UV cut-off effects seems mandatory. Moreover, simulations in the quenched approximation have shown that this improvement helps to extract the continuum limit also in the intermediate T range between 2 and $4T_c$.

The results of a computation of the pressure with an improved action in the gauge as well as in the fermion sector [16] are shown in figure 3. The data have been obtained for two- and three-light quarks with (bare) mass $m_q/T = 0.4$ as well as for two light quarks and a heavier one of mass $m_q/T = 1$. On the left side the pressure is shown in temperature units. Quite clearly, the pressure rises when the number of degrees of freedom increases. As in the quenched case, up to the highest temperature investigated it deviates substantially from the ideal gas behavior shown as the arrows to the right of the plot. The deviation is too big

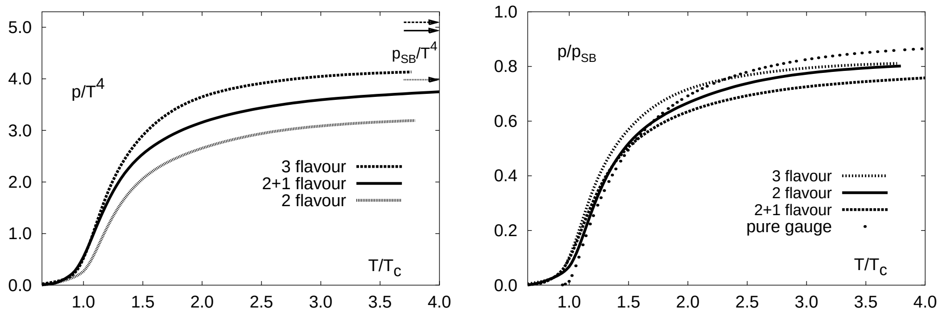

Figure 3. The pressure in QCD with two- and three-light quark flavors as well as with two light and one heavier quark. The computations have been carried out on lattices with temporal extent $N_\tau = 4$. The left plot shows the pressure in units of temperature while on the right side the data are normalized to the Stefan–Boltzmann limit. The right figure also includes the continuum extrapolated quenched result normalized to p_{SB}.

to be reproduced in ordinary high-temperature perturbation theory which converges badly in this temperature range. However, it is accounted for in quasi-particle models [17] and resummed perturbative approaches [18].

The results on the right-hand side of figure 3 have been normalized to the infinite temperature ideal gas Stefan–Boltzmann limit taking the non-vanishing quark mass into account. For comparison the right figure also includes the continuum extrapolated quenched result. The figure shows that, when plotted as a function of T/T_{c}, the pressure normalized to the Stefan–Boltzmann value is almost flavor-independent. Apart from a slight deficiency for the $2+1$ flavor case which may hint towards a less significant contribution from the would-be strange quarks the ideal gas limit thus correctly describes the liberation of partonic degrees of freedom

$$\frac{p}{T^4} = \left(16 + \frac{21}{2} N_{\mathrm{F}}\right) \times f(T/T_{\mathrm{c}})$$

corrected, however, by an apparently flavor independent function $f(T/T_{\mathrm{c}})$. At this stage it should be pointed out that the full QCD results have not yet been extrapolated to the continuum limit. However, the experience gathered perturbatively and in the quenched approximation leads one to expect that the finite a effects will distort these findings by not more than 10%.

The most recent results on the energy density are shown in figure 4. The staggered results on the left [19] have again been obtained for two-, three- and $2+1$-flavors on $N_\tau = 4$ lattices at the same mass values as given above. In the plot, a contribution which is proportional to the quark mass and vanishes in the chiral limit has been omitted. The Wilson data on the right [20] are for $N_{\mathrm{F}} = 2$ on $N_\tau = 4$ and 6 lattices. Note that the dependence on the quark mass appears to be rather weak over a wide range of values. Both data sets have been generated with improved actions. However, in the Wilson case the improvement does not reduce the infinite temperature finite lattice spacing effects. This is visible in the figure by the big difference in the Stefan–Boltzmann limits computed on the two lattices with differing N_τ values. On the other hand, the cut-off effects are not important close to T_{c} as a

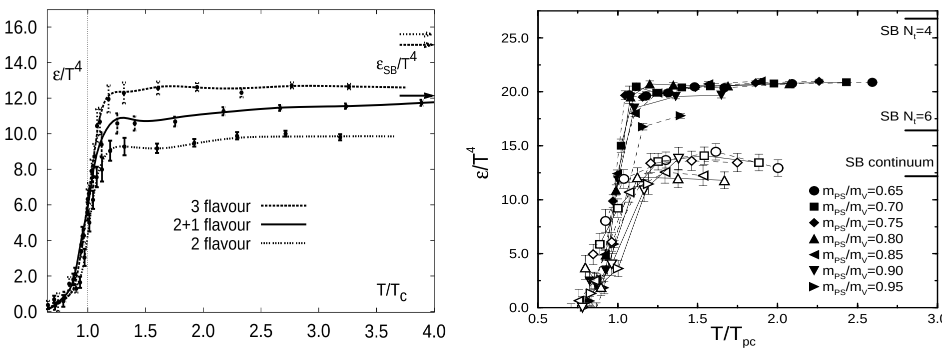

Figure 4. The energy density. The left figure shows results from improved staggered quarks on $N_\tau = 4$ lattices [19], the right one from two improved Wilson quarks on $N_\tau = 4$ (filled symbols) and $N_\tau = 6$ (open symbols) [20]. The marks on the right-hand side of the plots denote the Stefan–Boltzmann limits.

comparison between $N_\tau = 4$ and 6 results reveals. This is expected since in this temperature regime the correlation length is large and infra-red modes dominate. Thus, a comparison of the different fermion discretizations is meaningful and leads to the consistent result of $\varepsilon(T_\mathrm{c}) \simeq (6 \pm 2)T_\mathrm{c}^4$, which also agrees with the value originating from an earlier simulation with the standard staggered action [21].

4. Thermal hadron masses

Investigations into the nature of hadronic excitations are interesting for various reasons in the different temperature regimes. Below T_c temperature dependent modifications of hadron masses and widths may lead to observable consequences in heavy-ion collision experiments, e.g., a pre-deconfined dilepton enhancement. At temperatures around the transition temperature the (approach to the) restoration of chiral symmetry should reflect itself in degeneracies of the hadron spectrum. In the plasma phase the very nature of hadronic excitations is a question of interest. Asymptotic freedom leads one to expect that the plasma consists of a gas of free quarks and gluons. The lattice results on the equation-of-state, however, have shown already that this is not the case for the interesting temperature region. While quasi-particle models and HTL resummed perturbation theory are able to reproduce the equation-of-state it remains to be seen whether they also account properly for hadronic excitations. This question arises in particular as the generally assumed separation of scales $1/T \ll 1/gT \ll 1/g^2T$ does not hold for temperatures quite a few times T_c.

At zero temperature hadron masses and decay constants are obtained from amplitudes and exponential decreases of hadron correlation functions. At large separations between source and sink operator the two-point function is dominated by the ground state whose properties can then reliably be extracted. At finite temperature this approach is hampered by the fact that the temporal distance is limited by the inverse temperature, $0 \leq \tau \leq 1/T$. Therefore, most of the lattice studies have concentrated on the analysis of spatial correlation functions. In this case, the exponential decrease in the spatial distance is described by the screening mass.

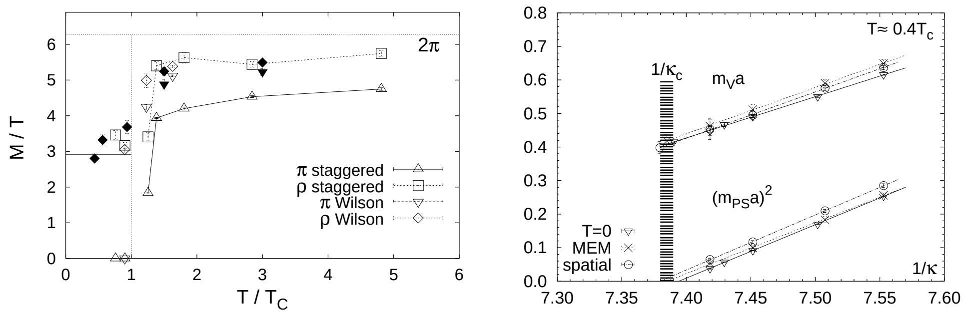

Figure 5. The left part shows screening masses in the quenched approximation [22] with preliminary Wilson fermion data [23] (filled symbols) added. Below T_c the masses are normalized to T_c, above to T. On the right, screening masses (spatial) are compared with masses (MEM, see below), both at $T = 0.4T_c$ [23], and with masses at $T = 0$ [24]. The data are plotted as a function of the quark mass, $m_q \sim 1/\kappa$, with the band indicating the chiral limit.

So far, below T_c the results do not show any significant temperature dependent difference between the screening masses and zero temperature masses. Above T_c one observes the degeneracy expected from chiral symmetry restoration. Also the difference between the pseudoscalar and scalar isovector channel diminishes indicating, for two quark flavors, the effective restoration of the anomalous $U_A(1)$. The values of the screening masses, in particular in the vector channel, approach the free quark propagation limit of $M_{\text{screen}} = 2\pi T$. The deviations from this value, however, hint towards important residual interactions. A representative set of these results in the quenched approximation [22,23] is shown in figure 5. To the left, screening masses are plotted in units of T_c below the critical temperature and in units of T above. On the right, screening masses are compared with masses, at zero [24] as well as at the same non-vanishing, albeit, with a value of $0.4T_c$ not very large temperature [23].

In order to study the temperature dependence of masses one has to analyze temporal correlations. Here, the use of anisotropic lattices [25] may help because the number of data points in the limited temporal interval is larger. However, one still has to rely on fit *ansätze* and, if possible, use the quality of the fit to distinguish between the various models. The full information about the existence of genuine hadron poles, their location and widths as well as other possible quasi-particle excitations is encoded in the spectral density $\sigma_H(\omega, \vec{p})$ in a given channel with the quantum numbers of a hadron H. At non-vanishing temperature, this quantity is related to the temporal correlation function $G_H(\tau, \vec{p})$ by

$$G_H(\tau, \vec{p}) = \int_0^\infty \mathrm{d}\omega \, \sigma_H(\omega, \vec{p}) \, \frac{\cosh(\omega(\tau - 1/(2T)))}{\sinh(\omega/(2T))}.$$

In general, extracting the continuous function σ from a limited number of discrete data points G is a so-called ill-posed problem. However, at $T = 0$, it could be demonstrated recently [26,27] that the use of the maximum entropy method [28], a refined statistical technique, indeed allows to determine the spectral density of hadron correlations. A first attempt [29] also proved successful at high temperature.

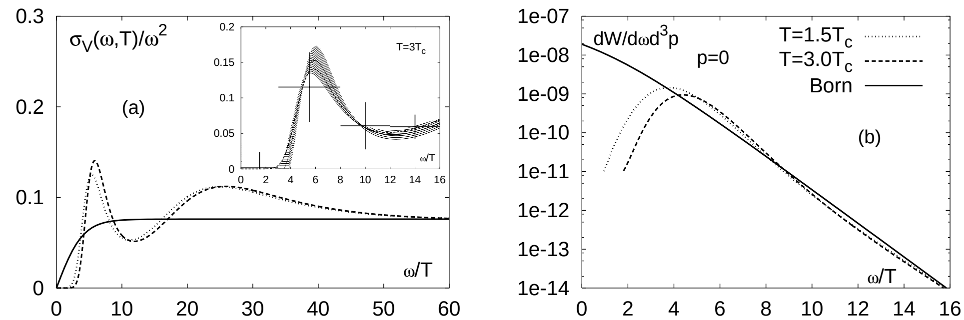

Figure 6. On the left side the vector spectral density, $\sigma_{\rm V} = \omega^2 \rho_{\rm V}$, at two temperatures $1.5T_{\rm c}$ and $3T_{\rm c}$ is compared with the free case. The inset shows the statistical error as a band and the MEM uncertainty as error bars in four different energy bins. The right part of the figure shows the resulting dilepton rate at $\vec{p} = 0$ compared with the Born rate.

The method is now being applied in an investigation of hadron correlators in the quenched approximation at various temperatures [23], first results of which are included in figure 5. A very interesting channel for a MEM analysis is the vector channel. Through the relation, for two-flavor QCD,

$$\frac{{\rm d}W}{{\rm d}\omega {\rm d}^3 p} = \frac{5\alpha^2}{27\pi^2} \frac{1}{\omega^2({\rm e}^{\omega/T} - 1)} \sigma_V(\omega, \vec{p}, T),$$

the spectral function $\sigma_{\rm V}$ in the vector channel is directly connected with the dilepton rate in heavy ion collisions [30]. At low energies, the dilepton rate is expected to be influenced by in-medium modifications of the quark–antiquark interactions. For instance, perturbative two-loop [31] as well as HTL-resummed [32] calculations lead to an enhancement of the spectrum at low energies, which dominates over the suppression arising from massive quasi-particle poles [30,32] or non-perturbative gluon condensates [33].

First lattice results [34] on the vector spectral density $\sigma_{\rm V}(\omega) = \omega^2 \rho(\omega)$ and the resulting dilepton rate at $\vec{p} = 0$ are shown in figure 6. The data have been obtained in the chiral limit at two temperatures above $T_{\rm c}$, $T = 1.5T_{\rm c}$ and $3T_{\rm c}$. The comparison with the free spectral density shows deviations by less than a factor 2 for energies $\omega \gtrsim 4T$. The broad enhancement at $\omega/T \gtrsim 20$ presumably is a lattice cut-off effect. The spectral density develops a peak around $\omega/T \simeq 5$ which seems to scale with the temperature. Compared to zero temperature results [26,27], the peak is rather broad in width and not very pronounced in height [35]. Nevertheless this peak leads to an enhancement of the dilepton rate in heavy ion collisions at these energies (see the right of the figure). The most prominent feature of the vector spectral function perhaps is the sharp drop at ω below $5T$ and a vanishing below $\omega \simeq 3T$. This effect is in contrast to e.g. HTL-resummed perturbation theory [32] which diverges in the zero energy limit. If this suppression persists in further studies and at temperatures closer to $T_{\rm c}$ there would be no thermal contribution to the dilepton rate at small energies during the expansion of the hot medium created in heavy-ion collisions.

5. Summary

The analysis of hot QCD including dynamical quarks by means of numerical lattice simulations is steadily progressing. Largely due to the use of improved actions the values for the critical temperature of the transition to the quark-gluon plasma are becoming conclusive. The critical properties of the transition could be clarified in the case of three-degenerate flavors while for two flavors and, even more so, for the physical case of two very light and one heavier quark further insight awaits more work. As in the pure gluon case, in the plasma phase the equation of state, i.e., energy density and pressure deviate substantially from a free gas picture. Unlike in the pure gluon case these bulk thermodynamic properties are, however, not yet available in the continuum limit, yet, the exploitation of improved actions leads one to expect that finite lattice spacing effects are not rendering the present results totally futile. The rediscovery of a refined statistical technique, the maximum entropy method, for lattice QCD has brought about new interesting results on the nature of hadronic excitations in the plasma. So far used only in the quenched approximation, without any model assumptions it has lend further support to observations that to first approximation hadronic correlations are close to free quark behavior, with evidence for remaining resonance-like structures at energies a few times the temperature. The deviations from free quark propagation led to an enhancement of dilepton rates at these and most likely to their suppression at smaller energies.

Acknowledgements

This work has been supported by the TMR network ERBFMRX-CT-970122 and by the DFG under grant FOR 339/1-2. Participation at the conference was made possible by the DFG under grant LA 784/6-1.

References

[1] R D Pisarski and F Wilczek, *Phys. Rev.* **D29**, 338 (1984)
[2] P Vranas, *Nucl. Phys. (Proc. Suppl.)* **B83-84**, 414 (2000)
[3] F Karsch and E Laermann, *Phys. Rev.* **D50**, 6954 (1994)
E Laermann, *Nucl. Phys. Proc. Suppl.* **60**, 180 (1998) and references therein
[4] S Aoki *et al*, (JLQCD Coll.), *Phys. Rev.* **D57**, 3910 (1998)
[5] C Bernard *et al*, *Phys. Rev.* **D61**, 054503 (2000)
[6] S Aoki *et al*, *Nucl. Phys. Proc. Suppl.* **63**, 397 (1998)
[7] J Engels *et al*, *Phys. Lett.* **B514**, 299 (2001)
[8] S Gavin, A Gocksch and R Pisarski, *Phys. Rev.* **D49**, 3079 (1994)
[9] F Karsch, E Laermann and Ch Schmidt, *Phys. Lett.* **B520**, 41 (2001)
[10] S Aoki *et al*, *Nucl. Phys. Proc. Suppl.* **73**, 459 (1999)
[11] F Karsch, E Laermann and A Peikert, *Nucl. Phys.* **B605**, 579 (2001)
[12] C Bernard *et al*, *Phys. Rev.* **D56**, 5584 (1997)
[13] A Ali Khan *et al*, *Phys. Rev.* **D63**, 34502 (2001)
[14] R G Edwards and U Heller, *Phys. Lett.* **B462**, 132 (1999)
[15] N Christ, private communication
[16] F Karsch, E Laermann and A Peikert, *Phys. Lett.* **B478**, 447 (2000)

[17] A Peshier *et al*, *Phys. Rev.* **D54**, 2399 (1996)
P Levai and U Heinz, *Phys. Rev.* **C57**, 1879 (1998)
[18] See the review by J-P Blaizot and E Iancu, hep-ph/0101103
[19] A Peikert, *Dissertation* (Bielefeld, 2000)
[20] A Ali Khan *et al*, *Phys. Rev.* **D64**, 074510 (2001)
[21] C Bernard *et al*, *Phys. Rev.* **D55**, 6861 (1997)
[22] E Laermann and P Schmidt, *Euro. Phys. J. C20*, 541 (2001)
[23] F Karsch *et al*, in preparation
[24] M Göckeler *et al*, *Phys. Rev.* **D57**, 5562 (1998)
[25] Ph de Forcrand *et al*, *Phys. Rev.* **D63**, 054501 (2001)
[26] M Asakawa, T Hatsuda and Y Nakahara, *Phys. Rev.* **D60**, 091503 (1999); *Prog. Part. Nucl. Phys.* **46**, 459 (2001)
[27] T Yamazaki *et al*, *Phys. Rev.* **D65**, 014501 (2002)
[28] M Jarell and J E Gubernatis, *Phys. Rep.* **269**, 133 (1996)
[29] I Wetzorke and F Karsch, *Proc. Int. Workshop on Strong and Electroweak Matter 2000*, hep-lat/0008008
[30] J Kapusta, *Phys. Lett.* **B136**, 201 (1984)
[31] T Altherr and P Aurenche, *Z. Phys.* **C45**, 99 (1989)
[32] E Braaten, R Pisarski and T Yuan, *Phys. Rev. Lett.* **64**, 2242 (1990)
P Aurenche *et al*, *Phys. Rev.* **D58**, 085003 (1998)
[33] M G Mustafa, A Schäfer and M H Thoma, *Phys. Rev.* **C61**, 24902 (2000)
[34] I Wetzorke *et al*, hep-lat/0110132
F Karsch *et al*, hep-lat/0110208
[35] Increased statistics could sharpen the peak [26] which would then be compensated by an even closer agreement with the free spectral function in other energy intervals [34]